International Journal of Thermophysics, Vol. 26, No. 1, January 2005 (© 2005)
DOI: 10.1007/s10765-005-2352-4

Viscosity and Liquid Density of Asymmetric *n*-Alkane Mixtures: Measurement and Modeling[1]

A. J. Queimada,[2,3] I. M. Marrucho,[3] J. A. P. Coutinho,[3] and E. H. Stenby[2,4]

Viscosity and liquid density measurements were performed, at atmospheric pressure, in pure and mixed *n*-decane, *n*-eicosane, *n*-docosane, and *n*-tetracosane from 293.15 K (or above the melting point) up to 343.15 K. The viscosity was determined with a rolling ball viscometer and liquid densities with a vibrating U-tube densimeter. Pure component results agreed, on average, with literature values within 0.2% for liquid density and 3% for viscosity. The measured data were used to evaluate the performance of two models for their predictions: the friction theory coupled with the Peng–Robinson equation of state and a corresponding states model recently proposed for surface tension, viscosity, vapor pressure, and liquid densities of the series of *n*-alkanes. Advantages and shortcoming of these models are discussed.

KEY WORDS: corresponding states; friction theory; liquid density; *n*-decane; *n*-docosane; *n*-eicosane; *n*-tetracosane; Peng–Robinson EOS; viscosity.

1. INTRODUCTION

Due to the vast number and nature of producing chemicals, the interest in asymmetric mixtures is emerging. These mixtures, containing lighter and heavier components, can easily be found among several industries such as those producing paints and polymers.

[1]Paper presented at the Fifteenth Symposium on Thermophysical Properties, June 22–27, 2003, Boulder, Colorado, U.S.A.

[2]Engineering Research Center IVC-SEP, Department of Chemical Engineering, Technical University of Denmark, Building 229, DK-2800 Kgs. Lyngby, Denmark.
[3]CICECO, Chemistry Department, Aveiro University, 3810-193 Aveiro, Portugal.
[4]To whom correspondence should be addressed. E-mail: ehs@kt.dtu.dk

Asymmetric systems are particularly important for the oil industry, since advances in the extraction technology due to the increasing depletion of oil reservoirs, are allowing for the additional recovery of heavier oil fractions, not extracted before, making the new oils more asymmetric. For the correct design of the extraction process, data or accurate models for their prediction are required. As the industrial interest in most of the heavier components was small until recently, the available experimental data are particularly scarce, and so the models for their prediction require additional evaluation before their application for these specific systems are performed.

This work is part of a broader project that involves measurement and modeling of the surface tension, viscosity, and liquid density of mixtures of a paraffin such as *n*-eicosane (*n*-$C_{20}H_{42}$), *n*-docosane (*n*-$C_{22}H_{46}$) or *n*-tetracosane (*n*-$C_{24}H_{50}$) with a smaller *n*-alkane, such as *n*-heptane (*n*-C_7H_{16}), *n*-decane ($C_{10}H_{22}$), or *n*-hexadecane (*n*-$C_{16}H_{34}$) [1–3].

Viscosity and liquid density are key properties in the design of oil extraction and petrochemical processes. In this paper, viscosity and liquid density measurements and modeling of three binary and one ternary mixtures are reported: *n*-decane + *n*-eicosane, *n*-decane + *n*-docosane, *n*-decane + *n*-tetracosane, and *n*-decane + *n*-eicosane + *n*-tetracosane.

2. EXPERIMENTAL

The following chemicals were used for the measurements with no further purification: *n*-decane (Aldrich, $\geq$ 99 mass%), *n*-eicosane (Aldrich, $\geq$ 99 mass%), *n*-docosane (Fluka, $\geq$ 98 mass%), and *n*-tetracosane (Fluka, $\geq$ 99 mass%). Mixtures were carefully prepared by weighing the components on a Sartorius analytical balance ($\pm$0.0001 g). After preparation, solutions were refrigerated between measurements.

An Anton Paar AMV 200 rolling ball microviscometer was used to obtain the viscosity results. This apparatus measures the time that a steel ball needs to roll down inside a glass capillary filled with sample. Combinations of ball/capillary of different diameters can be selected, giving a viscosity measuring range of 0.5–800 mPa · s, using very small amounts of sample (0.12–2.5 cm^3). A built-in temperature sensor, placed on a thermostatic capillary block on whose walls thermostatic water circulates, measures the temperature with an uncertainty of $\pm$0.01 K.

The viscosity is calculated from the liquid density and the rolling time using the following equation:

$$\eta = \kappa(\alpha) t \left(\rho_{\text{ball}} - \rho_{\text{liquid}}\right) \tag{1}$$

where η is the viscosity in mPa · s, κ is a calibration constant which only depends on the angle α, t is the rolling time, in s, and ρ is the density, in $kg \cdot m^{-3}$.

The parameter κ is only dependent on the angle, α, and has to be determined with liquids of known density and viscosity. Distilled water, along with Cannon Instruments Co. and HAAKE Medingen Gmbh standards, were used for the calibration and were selected so that the entire measuring range was covered.

Previous measurements in this viscometer have already shown the ability of this apparatus to measure viscosity accurately [1,4]. Other details about this equipment and the experimental procedure can be found elsewhere [1].

Liquid densities were determined in an Anton PAAR DMA 58 unit, based on the vibrating U-tube method. Air and degassed distilled water were used as calibration fluids. The temperature is kept constant with a built-in Peltier element and is displayed with a precision of ±0.01 K. Density values are displayed within $\pm 10^{-2}\,kg \cdot m^{-3}$.

Following the measurements, the viscometer capillary and the densimeter cell were carefully cleaned with toluene and ethanol. At the end they were dried with vacuum and compressed air, respectively.

3. MODELING

In this work, the friction theory viscosity model [1,5,6] coupled with the Peng–Robinson equation of state (PR EOS) [7] and a new three-reference fluid corresponding states model, previously developed to model liquid density, viscosity, vapor pressure, and surface tension of the series of the *n*-alkanes [8,9] will be evaluated for the estimation of the reported data.

3.1. f-Theory

In the friction theory the viscosity is modeled from a mechanical viewpoint, considering two contributions: one arising from the dilute gas and the other from the friction between layers, respectively, η_0 and η_f [1,6]:

$$\eta = \eta_0 + \eta_f \tag{2}$$

where η represents the viscosity, in mPa · s.

The dilute gas viscosity is calculated as a function of temperature, T/K, using the critical volume, $v_c/m^3 \cdot mol^{-1}$, the critical temperature, T_c/K, the molar mass, MW/$kg \cdot mol^{-1}$, and the acentric factor, ω [1,6]. The pure component friction contribution is related to the Peng–Robinson

EOS repulsive and attractive pressures by means of temperature-dependent friction coefficients, $\hat{\kappa}$.

$$\eta_f = \left[\hat{\kappa}_r \times \frac{p_r}{p_c} + \hat{\kappa}_{rr} \times \left(\frac{p_r}{p_c} \right)^2 + \hat{\kappa}_a \times \frac{p_a}{p_c} \right] \times \eta_c. \tag{3}$$

where p stands for the pressure (Pa), both subscripts r and rr represent repulsive, and c and a represent critical and attractive, respectively. η_c is a pure component characteristic critical viscosity for which the following equation was used [6]:

$$\eta_c = 3.8136 \times 10^{-8} p_c \mathrm{MW}^{0.601652} \tag{4}$$

The extension to mixtures follows from the properties of the pure components:

$$\eta_{mx} = \eta_{0_{mx}} + \eta_{f_{mx}} \tag{5}$$

$$\eta_{0_{mx}} = \exp\left[\sum_{i=1}^{n} x_i \ln\left(\eta_{0_i}\right) \right] \tag{6}$$

$$\eta_{f_{mx}} = \kappa_{r_{mx}} p_r + \kappa_{rr_{mx}} p_r^2 + \kappa_{a_{mx}} p_a \tag{7}$$

$$\kappa_{r_{mx}} = \sum_{i=1}^{n} z_i \frac{\eta_{c_i} \hat{\kappa}_{r_i}}{p_{c_i}} \tag{8}$$

$$\kappa_{rr_{mx}} = \sum_{i=1}^{n} z_i \frac{\eta_{c_i} \hat{\kappa}_{rr_i}}{p_{c_i}^2} \tag{9}$$

$$\kappa_{a_{mx}} = \sum_{i=1}^{n} z_i \frac{\eta_{c_i} \hat{\kappa}_{a_i}}{p_{c_i}} \tag{10}$$

$$z_i = \frac{x_i}{\mathrm{MW}_i^{0.3} \sum_{i=1}^{n} \frac{x_i}{\mathrm{MW}_i^{0.3}}} \tag{11}$$

where mx stands for a mixture property, n is the number of components, and x_i is the mole fraction of the ith component.

3.2. Corresponding States

Corresponding states models can be used to predict several equilibrium [8, 10–16] and transport properties [17, 18] over broad temperature and pressure conditions. In spite of its mathematical simplicity, corresponding

states, lies behind a strong theoretical basis and is able to produce very accurate predictions based on a small amount of experimental information.

In this work, a new corresponding states model [9] is extended for the prediction of the reported liquid densities and viscosities. Like the Teja approach [12,14,15,17], it is based on a Taylor series expansion of the evaluated reduced property (X_r) on the Pitzer acentric factor (ω), where the second (numerical) derivative (D_2) is also taken into account:

$$X_{\mathrm{r}} = X_{\mathrm{r}_1} + D_1(\omega - \omega_1) + D_2(\omega - \omega_1)(\omega - \omega_2) \tag{12}$$

$$D_1 = \frac{X_{\mathrm{r}_2} - X_{\mathrm{r}_1}}{\omega_2 - \omega_1} \quad D_2 = \frac{\frac{X_{\mathrm{r}_3} - X_{\mathrm{r}_1}}{\omega_3 - \omega_1} - \frac{X_{\mathrm{r}_2} - X_{\mathrm{r}_1}}{\omega_2 - \omega_1}}{\omega_3 - \omega_2} \tag{13}$$

The liquid density (ρ) and viscosity (η) are reduced using the following equations:

$$\rho_{\mathrm{r}} = V_{\mathrm{c}} \times \rho \quad \eta_{\mathrm{r}} = \frac{\eta \times V_{\mathrm{c}}^{2/3}}{\mathrm{MW}^{1/2} \times T_{\mathrm{c}}^{1/2}} \tag{14}$$

where T_{c}, V_{c}, and MW are the critical temperature in K, critical volume in $\mathrm{m}^3 \cdot \mathrm{mol}^{-1}$, and molar mass in $\mathrm{kg} \cdot \mathrm{mol}^{-1}$.

The extension to mixtures follows from the properties of the pure components:

$$\omega_{\mathrm{mx}} = \sum_i x_i \omega_i \tag{15}$$

$$V_{\mathrm{cmx}} = \sum_i \sum_j x_i x_j V_{\mathrm{c}ij} \tag{16}$$

$$T_{\mathrm{cmx}} V_{\mathrm{cmx}} = \sum_i \sum_j x_i x_j T_{\mathrm{c}ij} V_{\mathrm{c}ij} \tag{17}$$

$$V_{\mathrm{c}ij} = \frac{1}{8}(V_{\mathrm{c}i}^{\frac{1}{3}} + V_{\mathrm{c}j}^{\frac{1}{3}})^3 \tag{18}$$

$$T_{\mathrm{c}ij} = \sqrt{T_{\mathrm{c}i} T_{\mathrm{c}j}} \left(\frac{\sqrt{V_{\mathrm{c}i} V_{\mathrm{c}j}}}{V_{\mathrm{c}ij}} \right)^{(\frac{n}{3})-1} \tag{19}$$

where indexes i and j in the above equations represent pure components. The mixing rule for the critical temperatures, Eq. (19), where the exponent n can be used as a fitting parameter, replacing binary interaction parameters, was proposed by Coutinho et al. [19] and was previously successfully applied to model surface tensions of asymmetric *n*-alkane mixtures [3].

This model has already proved to be able to accurately predict vapor pressures, liquid densities, and viscosities of both lighter and heavier *n*-alkanes [9] and surface tensions of pure and mixed *n*-alkanes [2,3,8].

4. RESULTS AND DISCUSSION

In Tables I and II pure component results are compared with literature values [20–26]. Previous measurements on *n*-eicosane, *n*-docosane, and *n*-tetracosane, using the same equipment and reported elsewhere [1], are also included. Deviations less than 0.2% were found for the liquid densities. Viscosity deviations are higher, but still below 5% with the maximum deviation found for *n*-tetracosane, for which some experimental data are available. For the other *n*-alkanes average deviations are below 3%.

Mixture results are reported in Tables III and IV and shown on Figs. 1–4. No literature data were found for any of the mixture points. Maximum combined standard uncertainties were $0.003\,\mathrm{Kg}\cdot\mathrm{m}^{-3}$ for the liquid densities and $0.019\,\mathrm{mPa}\cdot\mathrm{s}$ for the measured viscosities, considering as components of uncertainty: composition, calibration of the apparatuses, temperature, rolling time (viscosity) and oscillating period (liquid density). With these results, liquid densities and viscosities of the $n\text{-}C_{10}H_{22} + n\text{-}C_{20}H_{42} + n\text{-}C_{24}H_{50}$ ternary and those of the corresponding binary (in terms of average chain length of the heavier components), $n\text{-}C_{10}H_{22} + n\text{-}C_{22}H_{46}$, can be compared, as already done for similar mixtures containing *n*-heptane, both for the reported properties [1] and surface tension [3]. Binary liquid densities showed a tendency to be slightly higher, although these differences are quite small, with deviations very close to zero (Fig. 4). On the other hand, as can be seen from Fig. 2, viscosities of the binary mixture tend to be higher, as previously found for the equivalent mixtures with *n*-heptane [1].

Modeling results are reported on Table V and Figs. 1 and 3. It is known that cubic equations of state, like the Peng–Robinson EOS, cannot provide accurate liquid density predictions of heavy hydrocarbons. Following the approach used before with the friction theory, critical parameters were fitted to the liquid densities [1] in order to better describe both the liquid densities and viscosities, since a good EOS pressure description is required within the f-theory. The fitted critical parameters are reported in Table VI. Table V shows how the Peng–Robinson EOS can now adequately represent liquid densities.

For the corresponding-states model, experimental critical properties were collected from the literature, when available [27]. Otherwise, previous assessed correlations were employed [8]. In Table V and Fig. 3 it is shown how this simple model can return liquid density estimates that deviate from

Table I. Pure Component Viscosities (in mPa · s) and Comparisons with Literature Results

n-alkane	*T*(K)	Exp.	DIPPR [20][a]	Wakefield et al. [21][b]	Ducoulombier et al. [26]	Cooper and Asfour. [24]	Vargaftik [22]	AAD (%)[c]
n-$C_{10}H_{22}$	293.2	0.899	0.913		0.924	0.9151	0.907	
	303.2	0.766	0.799					
	313.2	0.666	0.699		0.696			3.18
	323.2	0.587	0.610					
	333.2	0.522	0.543		0.546			
	343.2	0.472	0.487					
n-$C_{20}H_{42}$	313.2	4.01	4.06				4.072	
	323.2	3.20	3.26				3.259	2.02
	333.2	2.61	2.68				2.665	
	343.2	2.17	2.23				2.220	
n-$C_{22}H_{46}$	323.2	4.13						
	333.2	3.34						
	343.2	2.75						
n-$C_{24}H_{50}$	333.2	4.48	4.21	4.32				4.74
	343.2	3.67						
AAD (%)[c]			3.21	3.63	3.77	1.77	1.71	

[a] Average of reported experimental values.
[b] Interpolation of reported values at 328.16 and 338.16 K.
[c] $\text{AAD}\ (\%) = \frac{100}{n}\sum_{n}\frac{|x_{\text{measured}} - x_{\text{lit}}|}{x_{\text{lit}}}$

Table II. Pure Component Liquid Densities (in $kg \cdot m^{-3}$) and Comparisons with Literature Results

n-alkane	*T*(K)	Exp.	DIPPR [20][a]	Dutour et al. [23]	Vargaftik [22]	Cooper and Asfour [24]	Aralaguppi et al. [25]	AAD (%)[b]
n-$C_{10}H_{22}$	293.15	728.82	729.84		729.9	729.95		
	303.15	722.37	726.26		722.2		722.5	
	313.15	714.88	714.78		714.5			0.22
	323.15	707.12	713.13		706.7			
	333.15	699.41	699.63		698.9			
	343.13	691.61	697.58		691.0			
n-$C_{20}H_{42}$	313.15	775.13	775.89		775.6			
	323.15	768.33	769.17		769.0			0.10
	333.15	761.72	762.49		762.4			
	343.13	755.07	755.98		755.8			
n-$C_{22}H_{46}$	323.15	774.25	774.63					
	333.15	767.67	768.45					0.10
	343.13	761.12	762.24					
n-$C_{24}H_{50}$	333.15	772.72	772.81	773.77				
	343.13	766.24	766.25	766.66				0.05
AAD [b] (%)			0.24	0.10	0.07	0.15	0.02	

[a] Average of reported experimental values.

[b] $\text{AAD}\ (\%) = \frac{100}{n} \sum_{n} \frac{|x_{\text{measured}} - x_{\text{lit}}|}{x_{\text{lit}}}$.

Table III. Mixture Viscosities (in mPa · s)

Mixture	$x(1)$	$x(2)$	293.2 K	303.2 K	313.2 K	323.2 K	333.2 K	343.2 K
n-$C_{10}H_{22}$ (1) + n-$C_{20}H_{42}$ (2)	0.800	0.200	1.56	1.31	1.12	0.969	0.850	0.754
	0.600	0.400		2.01	1.68	1.42	1.23	1.07
	0.500	0.500		2.40	1.95	1.66	1.42	1.23
	0.400	0.600			2.38	1.96	1.68	1.44
	0.201	0.799			3.14	2.58	2.20	1.86
n-$C_{10}H_{22}$ (1) + n-$C_{22}H_{46}$ (2)	0.799	0.201		1.47	1.24	1.04	0.905	0.781
	0.600	0.400			2.05	1.71	1.45	1.26
	0.500	0.500			2.53	2.11	1.72	1.53
	0.400	0.600			2.93	2.43	2.04	1.74
	0.200	0.800				3.17	2.61	2.27
n-$C_{10}H_{22}$ (1) + n-$C_{24}H_{50}$ (2)	0.800	0.200			1.48	1.27	1.11	0.966
	0.601	0.399				2.09	1.78	1.53
	0.501	0.499				2.54	2.13	1.81
	0.400	0.600				3.11	2.59	2.18
	0.203	0.797				4.26	3.47	2.89
n-$C_{10}H_{22}$ (1) + n-$C_{20}H_{42}$ (2) + n-$C_{24}H_{50}$ (3)	0.801	0.100		1.43	1.20	1.03	0.896	0.789
	0.600	0.200			1.98	1.66	1.41	1.22
	0.504	0.248			2.36	2.00	1.69	1.45
	0.401	0.300				2.40	2.01	1.71
	0.203	0.395				3.22		2.22
	0.000	0.500				4.13	3.33	2.75

Table IV. Mixture Liquid Densities (in $kg \cdot m^{-3}$)

Mixture	$x(1)$	$x(2)$	293.15 K	303.15 K	313.15 K	323.15 K	333.15 K	343.13 K
n-$C_{10}H_{22}$ (1) + n-$C_{20}H_{42}$ (2)	0.800	0.200	748.59	741.43	734.23	726.82	719.47	712.13
	0.602	0.398		755.39	748.34	741.28	734.19	726.89
	0.500	0.500		761.50	754.51	747.44	740.49	733.52
	0.400	0.600			759.42	752.46	745.48	738.69
	0.201	0.799			768.00	761.15	754.34	747.66
n-$C_{10}H_{22}$ (1) + n-$C_{22}H_{46}$ (2)	0.799	0.201		744.68	737.51	730.24	722.95	715.69
	0.600	0.400			753.74	747.42	739.83	732.81
	0.500	0.500			759.50	752.95	746.11	739.29
	0.400	0.600			765.03	758.09	751.29	744.17
	0.200	0.800				767.13	760.49	753.93
n-$C_{10}H_{22}$ (1) + n-$C_{24}H_{50}$ (2)	0.800	0.200			740.97	733.76	726.59	720.06
	0.601	0.399				750.41	742.73	735.89
	0.501	0.499				757.19	750.04	742.22
	0.400	0.600				763.04	756.39	749.61
	0.203	0.797				772.16	765.65	759.08
n-$C_{10}H_{22}$ (1) + n-$C_{20}H_{42}$ (2) + n-$C_{24}H_{50}$ (3)	0.801	0.100		744.60	737.37	730.11	722.87	715.55
	0.600	0.200			753.40	746.44	739.30	732.32
	0.504	0.248			759.36	752.29	745.40	738.08
	0.401	0.300			764.90	758.10	751.60	744.40
	0.201	0.400				766.45	759.88	751.37
	0.000	0.500				774.31	767.69	760.43

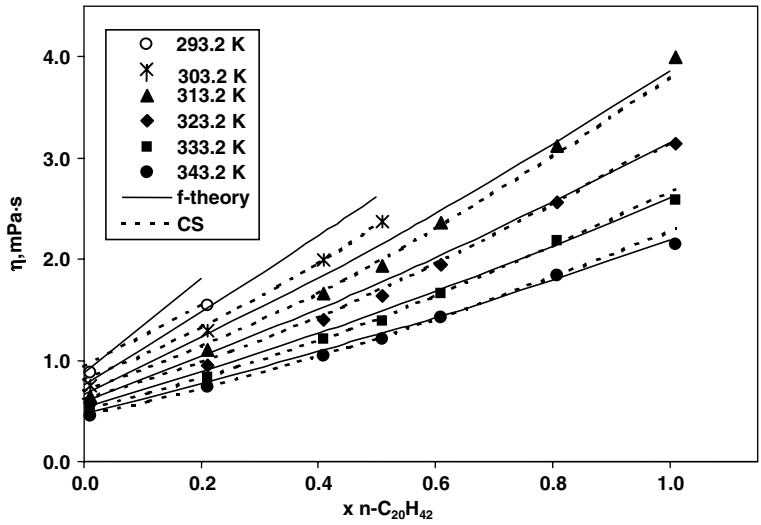

Fig. 1. Viscosity of the n-$C_{10}H_{22} + n$-$C_{20}H_{42}$ binary mixture. Experimental results and model predictions.

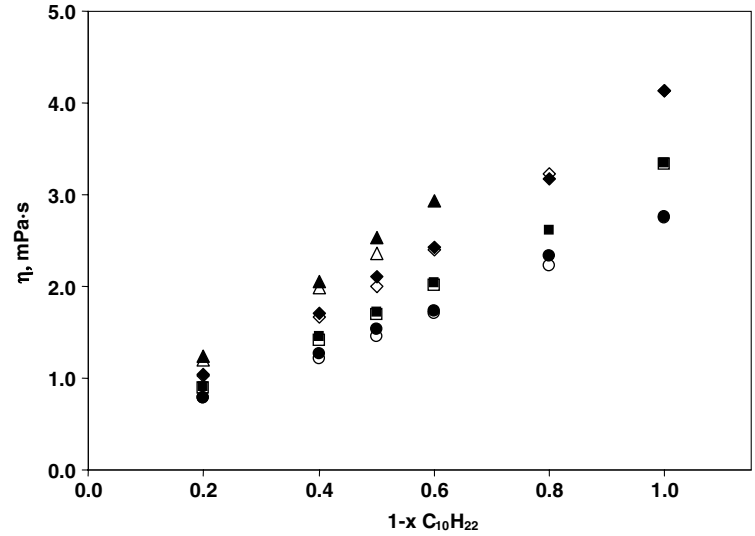

Fig. 2. Comparisons of the n-$C_{10}H_{22} + n$-$C_{22}H_{46}$ binary (closed symbols) and n-$C_{10}H_{22} + n$-$C_{20}H_{42} + n$-$C_{24}H_{50}$ ternary (open symbols) viscosity results. Triangles, 313.2 K; diamonds, 323.2 K; squares, 333.2 K; circles, 343.2 K.

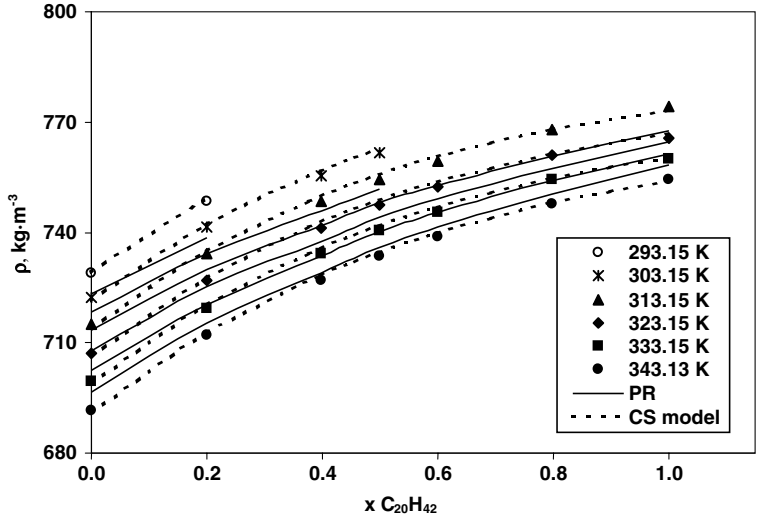

Fig. 3. Liquid density of the n-$C_{10}H_{22} + n$-$C_{20}H_{42}$ binary mixture. Experimental results and model predictions.

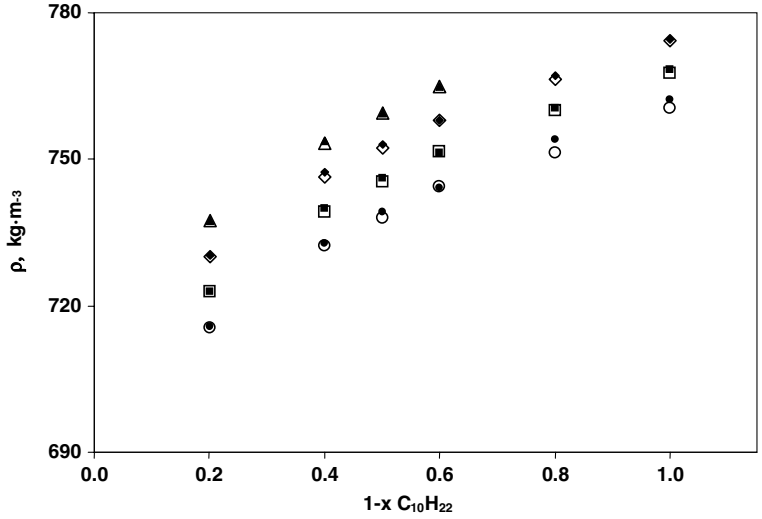

Fig. 4. Comparisons of the n-$C_{10}H_{22} + n$-$C_{22}H_{46}$ binary (closed symbols) and n-$C_{10}H_{22} + n$-$C_{20}H_{42} + n$-$C_{24}H_{50}$ ternary (open symbols) liquid density results. Triangles, 313.15 K; diamonds, 323.15 K; squares, 333.15 K; circles, 343.15 K.

Table V. Modeling Results with Pure Component Properties for the f-Theory and the PR EOS Reported in Table VI

	Average Absolute Deviation (AAD) (%)			
	Viscosity		Liquid density	
Mixture	f-theory	CS model	PR EOS	CS model
n-$C_{10}H_{22}$ + n-$C_{20}H_{42}$	4.2	2.3	0.52	0.13
n-$C_{10}H_{22}$ + n-$C_{22}H_{46}$	4.2	3.3	0.43	0.15
n-$C_{10}H_{22}$ + n-$C_{24}H_{50}$	3.8	7.9	0.37	0.21
n-$C_{10}H_{22}$ + n-$C_{20}H_{42}$ + n-$C_{24}H_{50}$	9.2	2.7	0.55	0.18
Average (all data points)	5.2	3.8	0.47	0.16

Table VI. Pure Component Properties Used Within the f-Theory and the PR EOS

n-alkane	T_c (K)	$P_c \times 10^{-5}$ (Pa)	$V_c \times 10^3$ ($m^3 \cdot mol^{-1}$)	ω	MW $\times 10^3$ ($kg \cdot mol^{-1}$)
n-$C_{10}H_{22}$	614.6	22.49	0.57326	0.49	142.285
n-$C_{20}H_{42}$	751.14	14.10	0.99043	0.865	282.554
n-$C_{22}H_{46}$	763.76	13.07	1.0624	0.963	310.607
n-$C_{24}H_{50}$	783.98	12.29	1.1334	1.032	338.661

the experimental data as much as different sets of data can deviate among themselves (Table II). The previously suggested reference system $CH_4 + C_{15}H_{32} + C_{26}H_{54}$ [9] was selected to obtain the reported results, using $n = 6$ in Eq. (19). As can be seen from the results, no need for further model refinement is required, and the model is predictive. For viscosity modeling of the reported asymmetric systems, an optimized n value is essential to reduce the absolute percent deviations below 10 %, but no need for system-dependent n-values was found. Using $n = -1.5$, very good viscosity predictions were obtained, as reported in Table V and Fig. 1, for the binary n-$C_{10}H_{22}$ + n-$C_{20}H_{42}$. Although typical n-values are in the range 3 to 7.5 [19], viscosity modeling using corresponding states theory with the one-fluid concept presents several simplifications, particularly for asymmetric mixtures, as discussed by Ely and Hanley [18]. Therefore, the optimized value of $n = -1.5$ accounts for these simplifications, and should thus be considered as a fitting parameter. Only binary mixture data were

used for the optimization. The previously suggested viscosity reference system, $C_2H_6 + C_8H_{18} + C_{18}H_{38}$, was selected to obtain the reported results [9].

Good viscosity predictions are obtained with the friction theory, with the largest deviations found for the ternary system, as previously noted [1]. However, it should be remembered that no mixture information was used in either the EOS or in the f-theory.

Within the same mixture, major deviations were found for both models at the lowest temperatures, where viscosity measurements are harder to perform, and thus more uncertain. At these temperatures, the PR EOS also showed the largest liquid density deviations, from which larger viscosity deviations may be expected from the f-theory.

5. CONCLUSION

Viscosity and liquid density data for three additional binary and one ternary *n*-alkane mixtures are presented. Comparisons with literature confirmed that our equipment can accurately determine liquid densities and viscosities with average deviations of 0.2% and 3%, respectively.

The measured properties of the ternary mixture, n-$C_{10}H_{22} + n$-$C_{20}H_{42} + n$-$C_{24}H_{50}$, were compared with those for the equivalent binary, n-$C_{10}H_{22} + n$-$C_{22}H_{46}$. Results confirmed a previous study where it was found that although the corresponding liquid densities can be considered equal, viscosities of the binary mixture tend to be higher.

The friction theory, in combination with the Peng–Robinson equation of state, and a corresponding states model were evaluated to describe the measured data. After fitting the pure component critical properties to improve the description of the liquid densities, a good representation of the viscosities resulted from the f-theory. Very good liquid density results were obtained from the corresponding states model. Viscosity predictions using this model require optimization of the cross-critical temperature combining rule, but by using a system-independent n parameter, very good results are obtained.

ACKNOWLEDGMENTS

A. J. Queimada thanks *Fundação para a Ciência e a Tecnologia* his Ph.D. scholarship BD/954/2000 and Fundação Calouste Gulbenkian for a conference scholarship. S. E. Quiñones-Cisneros is gratefully acknowledged for the help with the friction theory model. Dang Thuong is acknowledged for performing some of the reported experimental measurements.

REFERENCES

1. A. J. Queimada, S. E. Quinõnes-Cisneros, I. M. Marrucho, A.P. Coutinho, and Erling H. Stenby, *Int. J. Thermophys*. **24**:1121 (2003).
2. L. I. Rolo, A. I. Caço, A. J. Queimada, I. M. Marrucho, and J. A. P. Coutinho, *J. Chem. Eng. Data* **47**:1442 (2002).
3. A. J. Queimada, F. A. E. Silva, A. I. Caço, I. M. Marrucho, and J. A. P. Coutinho, *Fluid Phase Equilib*. **214**:211 (2003).
4. A. Y. Dandekar, S. I. Andersen, and E. H. Stenby, *J. Chem. Eng. Data* **43**:551 (1998).
5. S. E. Quiñones-Cisneros, C. K. Zéberg-Mikkelsen, and E. H. Stenby, *Fluid Phase Equilib*. **169**:249 (2000).
6. S. E. Quiñones-Cisneros, C. K. Zéberg-Mikkelsen, and E. H. Stenby, *Fluid Phase Equilib.* **178**:1 (2001).
7. D. Y. Peng and D. B. Robinson, *Ind. Eng. Chem. Fund.* **15**:59 (1974).
8. A. J. Queimada, I. M. Marrucho, and J. A. P. Coutinho, *Fluid Phase Equilib.* **183–184**:229 (2001).
9. A. J. Queimada, E. H. Stenby, I. M. Marrucho, and J. A. P. Coutinho, *Fluid Phase Equilib*. **212**:303 (2003).
10. B. E. Poling, J. M. Prausnitz, and J. P. O'Connell, *The Properties of Gases and Liquids*, 5th Ed. (McGraw-Hill, New York, 2000).
11. D. L. Morgan and R. Kobayashi, *Fluid Phase Equilib*. **94**:51 (1994).
12. A. S. Teja, S. I. Sandler, and N. C. Patel, *Chem. Eng. J.* **21**:21 (1981).
13. K. S. Pitzer, D. Z. Lippmann, R. F. Curl, C. M. Huggins, and D. E. Petersen, *J. Am. Chem. Soc.* **77**:3433 (1955).
14. A. S. Teja, *AIChE J.* **26**:337 (1980).
15. P. Rice and A. S. Teja, *J. Colloid Interf. Sci.* **86**:158 (1982).
16. Y. Zuo and E. Stenby, *Can. J. Chem. Eng.* **75**:1130 (1997).
17. A. S. Teja and P. Rice, *Chem. Eng. Sci.* **36**:7 (1981).
18. J. F. Ely and H. J. M. Hanley, *Ind. Eng. Chem. Fund.* **20**:323 (1981).
19. J. A. P. Coutinho, P. M. Vlamos, and G. M. Kontogeorgis, *Ind. Eng. Chem. Res.* **39**:3076 (2000).
20. Design Institute for Physical Property Data, *DIPPR Database*, AIChE, New York (1998).
21. D. L. Wakefield, K. N. Marsh, and B. J. Zwolinski, *Int. J. Thermophys.* **9**:47 (1988).
22. N. B. Vargaftik, *Tables on the Thermophysical Properties of Liquids and Gases – in Normal and Dissociated States*, 2nd Ed. (John Wiley, New York, 1975).
23. S. Dutour, B. Lagourette, and J. Daridon, *J. Chem. Thermodyn.* **33**:765 (2001).
24. E. F. Cooper and A. Asfour, *J. Chem. Eng. Data* **36**:285 (1991).
25. M. I. Aralaguppi, C. V. Jadar, and T. M. Aminabhavi, *J. Chem. Eng. Data* **44**:435 (1999).
26. D. Ducoulombier, H. Zhou, C. Boned, J. Peyrelasse, H. Saint-Guirons, and P. Xans, *J. Phys. Chem.* **90**:1692 (1986).
27. D. Ambrose, and C. Tsonopoulos, *J. Chem. Eng. Data* **40**:531 (1995).